RSC Advances

PAPER

View Article Online
View Journal | View Issue

Cite this: *RSC Adv.*, 2019, **9**, 41287

Preparation and *in vitro* bioactivity evaluation of N-heterocyclic-linked dihomooxacalix[4]arene derivatives†

Lin An, *[ab] Jia-dong Liu,[ab] Xian-na Peng,[a] You-guang Zheng,[ab] Chan Wang[ab] and Tong-hui Huang[ab]

Based on the superior prospects of calixarenes-based agents and N-heterocyclic pharmacophores in biomedical applications, 14 new dihomooxacalix[4]arene N-heterocyclic (pyridine, quinoline, and thiazole) derivatives **4a–4n** were efficiently synthesized from the parent compound, namely, *p*-*tert*-butyldihomooxacalix[4]arene **1**; they were further investigated by using their IR, ^{1}H NMR, ^{13}C NMR, and HRMS spectra. Among these derivatives, the crystal and molecular structures of 2-aminomethylpyridine-substituted dihomooxacalix[4]arene **4f** (obtained from methanol) have been determined by X-ray diffraction. In the case of the inhibition assay of cell growth, we evaluated the effects on four select tumor cell lines (MCF-7, HepG2, SKOV3, and HeLa), as well as the normal cell lines of HUVEC, using paclitaxel as the positive control drug. It was found that the derivatives **4d–4f**, **4i**, **4k**, and **4l** could inhibit tumoral activity up to varying degrees. Mechanistically, the cell cycle analysis demonstrated that dihomooxacalix[4]arene N-heterocyclic derivatives could induce apoptosis of MCF cells. In addition, the results of the western blot and immunofluorescence studies revealed the upregulation of the protein expression levels of Bax and cleaved caspase-3, as well as the downregulation of Bcl-2, which are in good agreement with the corresponding inhibitory potencies. Therefore, these findings suggest that N-heterocyclic derivatives based on the dihomooxacalix[4]arene scaffold are promising candidates for use against cancer.

Received 29th August 2019
Accepted 22nd November 2019

DOI: 10.1039/c9ra06876g

rsc.li/rsc-advances

Introduction

From the past several decades, cancer has been predominantly considered to be one of the most critical health problems worldwide. Recently, the International Agency for Research on Cancer (IARC) reported that in 2018, the number of new cancer cases is expected to reach 18.1 million and cancer deaths reaching 9.6 million.[1] Research on designing anticancer agents is also growing fairly rapidly and broadly, leading to drug diversity.[2] It is well known that conventional chemotherapy based on synthetic drugs has occupied a critical position in the treatment of cancer.[3] However, it suffers from severe non-selectivity, drug resistance, and other side-effects.[4] In this way, cancer research is still a formidable challenge.

With regard to conventional chemotherapy, supramolecular chemotherapy can prove to be a highly promising candidate because it can resolve the drawbacks of traditional chemotherapy by using host–guest interactions such as π–π stacking effects, electrostatic interactions, and hydrogen bonding interactions with small drug molecules.[5] Calixarenes—the third generation of supramolecules—are an important class of cyclic oligomers formed by the condensation of multiple phenol units and formaldehyde under alkaline conditions.[6] In the last few decades, owing to their flexible conformations, variable cavity dimensions, easy modifications, and limited toxicity and immune responses, research on the therapeutic applications of calixarenes and their derivatives has formed an emerging area of interest.[7] A large number of calixarene derivatives have been reported as drug building blocks.[8]

It has been proven that N-heterocyclic compounds, such as quinoline, pyridine, pyrimidine, anthraquinone, benzimidazole, and so on, have high efficiency and enhanced structural diversity, because of which they have become a research hotspot in the field of pesticides and medicines.[9] Many natural products (*e.g.*, camptothecin, reserpine, and analgesic morphine) or chemically synthesized drugs have exhibited biological activity mainly due to the presence of N-heterocyclic groups.[10] The introduction of N-heterocyclic units in well-defined calixarene scaffolds has been proven to be feasible and useful. For example, quinoline–pyrimidine-linked calix[4]arene scaffolds exhibited worthwhile antimalarial activity against the *P.*

[a]*College of Pharmacy, Xuzhou Medical University, Xuzhou 221004, P. R. China. E-mail: anlinhx@xzhmu.edu.cn*

[b]*Jiangsu Key Laboratory of New Drug Research and Clinical Pharmacy, Xuzhou Medical University, Xuzhou 221004, P. R. China*

† Electronic supplementary information (ESI) available. See DOI: 10.1039/c9ra06876g

falciparum strain.[11] Further, 8-oxyquinolinepropoxycalix[4]arene and 5-Cl-8-oxyquinolinepropoxycalix[4]arene exerted antifungal activity against *C. albicans*.[12] In addition, pyrrolidine-appended calix[4]arene exhibited excellent antifungal action toward *A. niger*.[13] Homooxacalixarenes are an analog of calixarenes,[14] where the methylene groups (–CH_2–) are partially or totally replaced by the oxypropylene group (–CH_2OCH_2–). They have improved conformational mobility and structural flexibility characteristics; moreover, they are much more suitable for use in an interesting framework for the new drug design of a molecular platform. In the present work, we are interested to formulate the pyridine, quinoline, or thiazole groups *via* the amido acetoethoxy spacer to the lower rim of dihomooxacalix[4]arene to afford novel N-heterocyclic-amido-attached dihomooxacalix[4]arene derivatives. Further, the antitumor effects of these compounds on breast (MCF-7), liver (HepG2), ovarian (SKOV3), and cervical (HeLa) cancer cells were evaluated, as well as the possible mechanisms were discussed.

Results and discussion

Synthesis and characterization

The synthesis strategy for dihomooxacalix[4]arene N-heterocyclic derivatives **4a–4n** are shown in Scheme 1.

Evidently, compounds **4a–4n** were synthesized starting from *tert*-butyl dihomooxacalix[4]arene **1**.

For attaching the N-heterocyclic units to the lower rim of the dihomooxacalix[4]arene scaffold, we initially introduced ester groups to form an acetoethoxy spacer using a moderate condition similar to the procedures reported by Marcos and us.[8d,15,16] We found that compound **1** easily reacted with ethyl 2-bromoacetate and potassium carbonate at a molar ratio of 1 : 2 : 12 in refluxing acetone, yielding a mixture of nearly 1 : 1 mono and 1,3-disubstituted ester **2a** and **2b**, which were separated and purified by silica gel column chromatography (4 : 1 v/v, petroleum ether/ethyl acetate). The further reaction of ester **2a** or **2b** with excess 4-aminomethylpyridine was carried out at the ambient temperature. The consequent reaction was rapid and

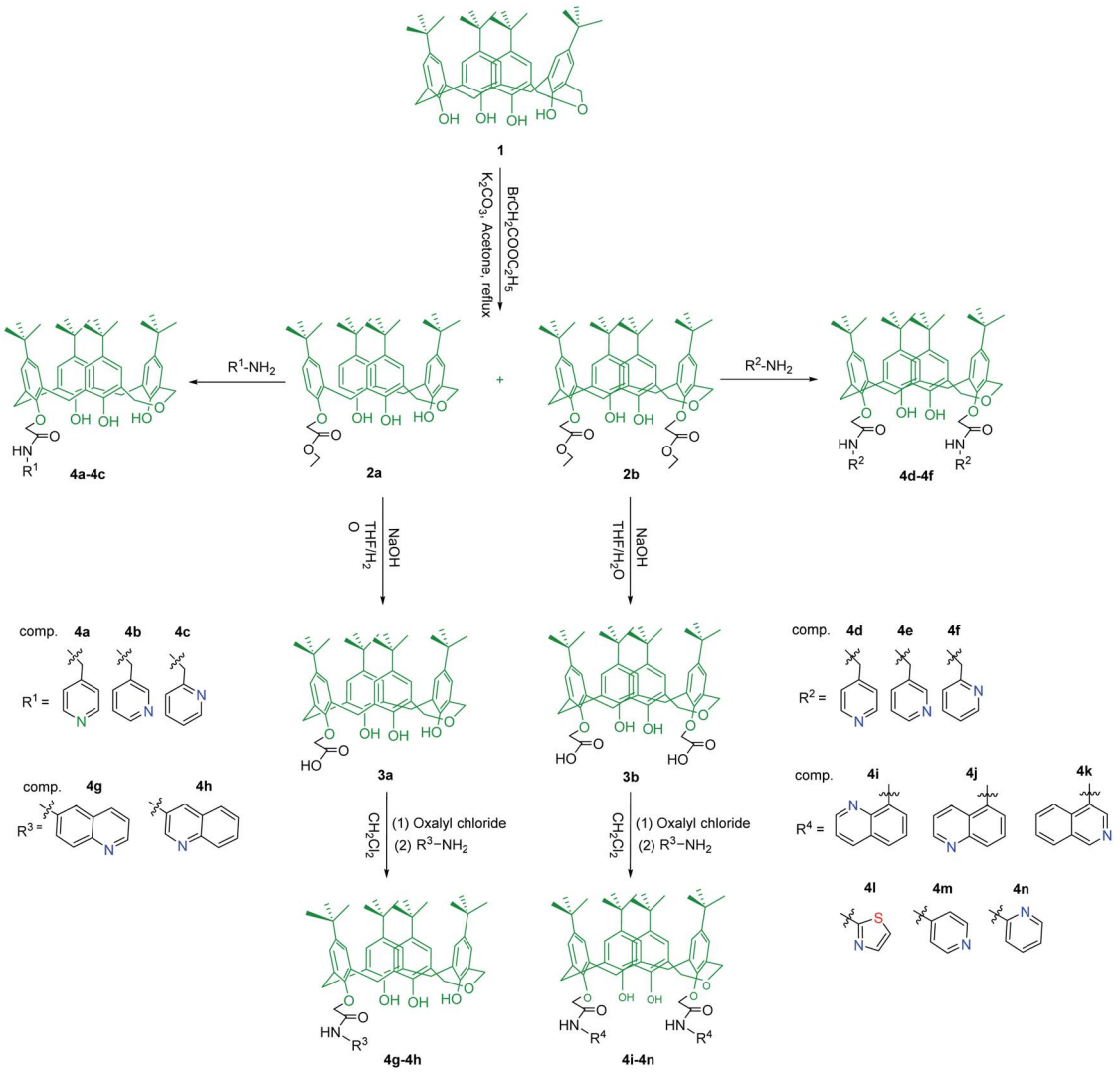

Scheme 1 Synthesis of dihomooxacalix[4]arene N-heterocyclic derivatives **4a–4n**.

the corresponding products of **4a** and **4d** were readily obtained in the form of white solids in good yields of 90.1% and 93.2%, respectively. In addition, the analogs of the above compounds bearing 3- or 2-aminomethyl pyridine moieties (**4b–4c**; **4e–4f**) were yielded varying from 82.9% to 94.5%. However, the same reaction, when conducted with 4-aminopyridine, hardly proceeded and failed to yield the expected compound with more hindrance and less activity, regardless of improving the reaction conditions. Hydrolysis was subsequently conducted by the treatment of intermediates **2a** and **2b** with sodium hydroxide in aqueous THF to yield carboxylic acids **3a** and **3b**, respectively. Thereafter, carboxylic acid formed into acid chloride, followed by amidation with amino-N-heterocyclic compounds in dry THF in an ice bath for 24 h, affording **4g–4n** in a quantitative yield.

Such synthetic dihomooxacalix[4]arene N-heterocyclic derivatives **4a–4n** have not been reported before; their structures were confirmed from their ^{1}H NMR, ^{13}C NMR, and HRMS spectra. As expected, the ^{1}H NMR spectra of **4a** exhibited three single signals at 8.86, 8.49, and 7.80 ppm for protons of the unreacted free phenolic hydroxyl groups. A triple singlet for the protons of the –NH– group appeared at 9.31 ppm. Aromatic protons appeared at 7.28, 7.16, 7.12–7.14, 7.09, 6.93, and 6.91 ppm for the complicated characteristic resonances. In addition, the chemical shift at 8.53 (d) and 7.39 (d) ppm, arose from the aminomethyl pyridine ring, further revealing the successful preparation of **4a**.

X-ray crystal structure of 4f

The X-ray crystal structure of derivative **4f** was determined, as shown in Fig. 1.

As shown in Fig. 1, dihomooxacalix[4]arene derivative **4f** possesses a cone conformation, where the two 2-aminomethyl pyridyl-carbonyl methoxyl substitutes are in the 1,3-alternate position at the lower rim of the macrocyclic ring. This belongs to the monoclinic space group of *C*2/*c*. The X-ray structure of **4f** also reveals that one of the aromatic rings constructed by C2, C3, C4, C5, C6, and C7 atoms is nearly parallel to the mean plane defined by O2, O3, O5, and O6 phenolic oxygen atoms. The corresponding dihedral angle between the mean plane and this ring is 20.630° (53). The other three aromatic rings, bearing O3, O5, and O6 atoms, have the dihedral angles of 77.448° (66), 54.353° (57), and 53.698° (53), respectively. In addition, in the molecule of **4f**, the two pyridine rings exist on the same side of the dihomooxacalix[4]arene and are constrained to be roughly parallel to each other. The N2 and N4 atoms in the pyridine rings are, therefore, located at slightly longer distances of 8.2457 Å (48), which provides further stabilization.

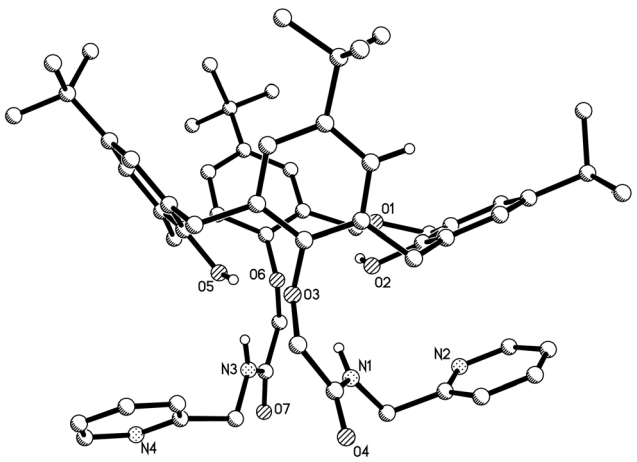

Fig. 1 Molecular structure of **4f** (hydrogen atoms are omitted for clarity; displacement ellipsoids are drawn at the 30% probability level).

Cytotoxicity assay

To determine the effect of dihomooxacalix[4]arene N-heterocyclic derivatives **4a–4n** on cell cytotoxicity, the cell viabilities of these compounds were assessed by the MTT reduction assay. Initially, we investigated the single-concentration inhibition rate after 72 treatments (concentration: 15 μM) against 4 different cell types: MCF-7, HepG2, SKOV3, and HeLa cells. The results are listed in Table 1.

N-Heterocyclic rings, *e.g.*, a quinoline scaffold, have always attracted attention and played important roles in the development of drugs because of their anticancer, antimicrobial, and antimalarial activities.[9e,17] Abouzid and coworkers prepared 6-alkoxy-4-substituted-aminoquinazolines and exploited the potent antitumor activity toward MCF-7 cells with IC_{50} values in the nanomolar range.[18] In our design, pyridine, quinoline, and thiazole were introduced in the dihomooxacalix[4]arene platform by using a linker in the form of an acetoethoxy spacer at the lower rim. The cell cytotoxicity results of the synthetic derivatives of **4a–4n** (Table 1) showed that nearly all the mono-aminomethyl-pyridine- and quinoline-substituted dihomooxacalix[4]arene derivatives exhibited weak effects on the four tested cancer cells, except **4h** toward SKOV3 cells (73%). In contrast, a majority of 1,3-di-N-heterocyclic-substituted dihomooxacalix[4]arene derivatives exhibited effective improvements in cell inhibition. For example, 1,3-di-4-aminomethyl pyridine derivatives **4d** showed

Table 1 Single-concentration inhibition of compounds **4a–4n** (concentration: 15 μM)

	Single concentration inhibition (%)				
Compd	MCF-7	HepG2	SKOV3	HeLa	HUVEC
4a	26	37	35	27	12
4b	25	29	52	39	15
4c	14	26	35	40	18
4d	96	66	69	64	25
4e	95	94	83	64	33
4f	67	94	54	50	16
4g	<0	30	44	38	34
4h	<0	24	73	38	<0
4i	24	26	39	71	23
4j	23	25	50	18	<0
4k	94	91	75	82	27
4l	89	16	40	54	43
4m	26	22	36	39	24
4n	23	26	48	28	31

Table 2 IC_{50} values (μM) of dihomooxacalix[4]arene-based compounds on cell viability[a]

	IC_{50} (μM)			
Compd	MCF-7	HepG2	SKOV3	Hela
4d	1.2 ± 0.2	17.6 ± 1.2	3.8 ± 0.9	3.9 ± 0.6
4e	4.1 ± 0.8	8.8 ± 0.8	5.8 ± 0.9	7.9 ± 1.0
4f	5.4 ± 0.3	22.7 ± 3.0	NT	10.9 ± 1.5
4h	NT	NT	7.6 ± 0.4	NT
4i	NT	NT	NT	7.3 ± 0.8
4k	3.7 ± 1.3	2.3 ± 0.4	3.5 ± 0.8	6.0 ± 1.7
4l	2.7 ± 0.3	NT	NT	NT
Paclitaxel	(1.7 ± 0.8) nM	(1.5 ± 0.2) nM	(3.8 ± 1.2) nM	(3.0 ± 1.0) nM

[a] "NT" means not detected.

a significant effect on MCF-7 cells with single-concentration inhibition of 96%. Derivative **4e** had worthwhile inhibition rates of 95%, 94%, 83%, and 64% on MCF-7, HepG2, SKOV3, and HeLa cells. Interestingly, the obtained results are similar to those of 1,3-di-3-aminoquinoline-substituted derivative **4k**, where the inhibition cancer cells ranged from 75% to 94%. As expected, **4k** also exhibited low toxicity toward HUVEC cells (inhibition: 27%). The differences in the inhibition activities of **4a–4n** reveal that the numbers, kinds, and positions of the N-heterocyclic groups may have a definite influence on the activity. Further, it was noted that our design of N-heterocyclic compounds was not based on a clear target. Therefore, we could only speculate that such an influence may be attributable to the conjugate effect and steric hindrance of N-heterocyclic rings with an acylamino spacer.

According to the preliminary screening results, the cytotoxic activities (IC_{50} values) of select compounds with single-concentration inhibition rates in excess of 50% are listed in Table 2.

Overall, they exhibited strong cytotoxic effects (IC_{50} values ranging from 1.2 ± 0.2 μM to 22.7 ± 3.0 μM) against all the four types of cancer cells. These preliminary results tend to confirm that 1,3-di-N-heterocyclic dihomooxacalix[4] derivatives have efficient antitumor activity, which encouraged us to mechanically perform the molecular studies.

Morphological observation

MCF-7 cells were treated with different concentrations (0, 10, and 20 μM) of dihomooxacalix[4]arene N-heterocyclic derivative **4k** for 24 h and then photographed by an inverted optical microscope. The morphological changes are shown in Fig. 2.

Evidently, the cell morphology significantly changed as the drug concentration increased as compared to that of the control group. When the concentration was 20 μM, a large number of cells became spherical and got separated from the surface of the culture dish, indicating that cell proliferation was inhibited.

Western blotting assay

As a pro-apoptotic protein in the Bcl-2 family, Bax over-expression in cells can antagonize the expression of Bcl-2, leading to apoptosis. Therefore, the relative expression levels of Bax and Bcl-2 can be used as the apoptotic signals of cells. In addition, caspase-3 is a vital executioner molecule during the apoptotic process.[19] In this work, in order to qualitatively determine whether **4k** had an apoptotic effect on MCF-7 cells, the expression levels of various apoptosis-related proteins in MCF-7 cells induced by different concentrations of **4k** (0, 10, and 20 μM) were detected by immunoblotting. The results are shown in Fig. 3.

As shown in Fig. 3, with an increase in the concentration of administration, the expression levels of Bcl-2 and Bax were negatively and positively correlated with the dose, respectively; Bax concentration gradually increased. It should be noted that cleaved caspase-3 usually acted as the key protein for pro-apoptosis and its expression level increased, indicating that **4k** could promote the apoptosis of MCF-7 cells.

Immunofluorescence assay

To further elucidate the apoptotic effect of **4k** on MCF-7 cells, the expression levels of the related apoptotic proteins were evaluated by immunofluorescence staining. After the treatment

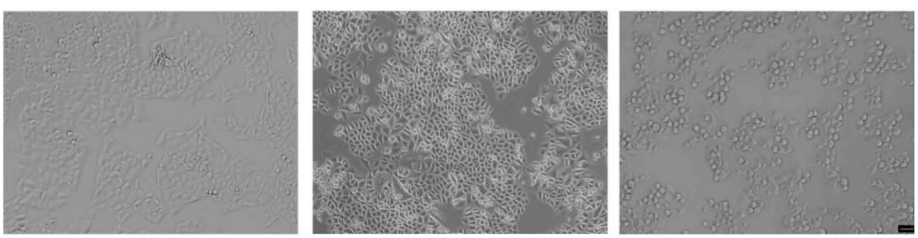

Fig. 2 Cell morphological changes observed under an inverted optical microscope. Scale: 10 μm.

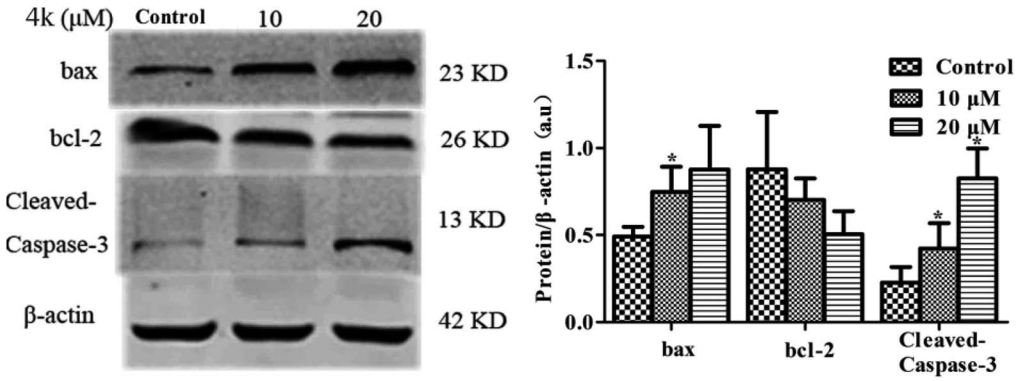

Fig. 3 Effects of **4k** on the apoptotic protein expressions in MCF-7 cells. The protein bands of Bax, Bcl-2, cleaved caspase-3, and β-actin in MCF-7 cells were determined by western blotting; β-actin was used as the internal standard for each sample. Relative levels of Bax, Bcl-2, and cleaved caspase-3 in MCF-7 cells performed by densitometric analysis. *$P < 0.05$ *vs.* the control group.

of MCF-7 cells with different concentrations of **4k** (0, 10, and 20 μM) for 24 h, the Bcl-2 and cleaved caspase-3 antibodies were added at 4 °C overnight, the fluorescent secondary antibody was incubated, the nucleus was stained with DAPI, and the cells were mounted and observed using an inverted fluorescence microscope. The results are shown in Fig. 4.

From Fig. 4, it is evident that as the drug concentration increases, the fluorescence intensity of Bcl-2 gradually decreases, and the fluorescence intensity of cleaved caspase-3 gradually increases. This result is consistent with the immunoblotting data, further indicating that **4k** could promote the apoptosis of MCF-7 cells.

Flow cytometry assay

In order to quantitatively determine the apoptotic rate of MCF-7 cells induced by **4k**, flow cytometry was used for the detection; the results are shown in Fig. 5.

It is well known that cells are divided into four subgroups, namely, Q1, Q2, Q3, and Q4, where the proportions of cells in Q2 and Q3 are used to reveal the overall apoptosis of cells. As

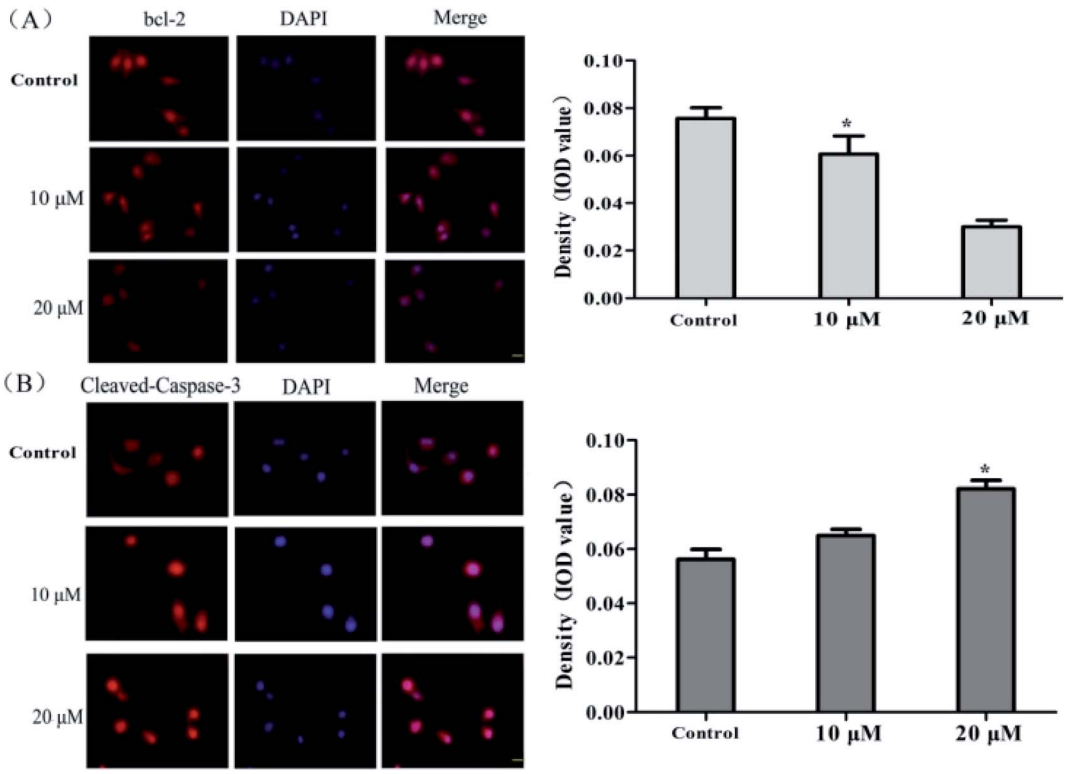

Fig. 4 Effects of **4k** on the apoptotic protein expressions in MCF-7 cells. (A) Bcl-2 and (B) cleaved caspase-3 protein antibodies and fluorescein-conjugated second antibody were used to visualize the corresponding protein; DAPI was used to stain the cell nuclei (blue). Scale: 10 μm. *$P < 0.05$ *vs.* the control group.

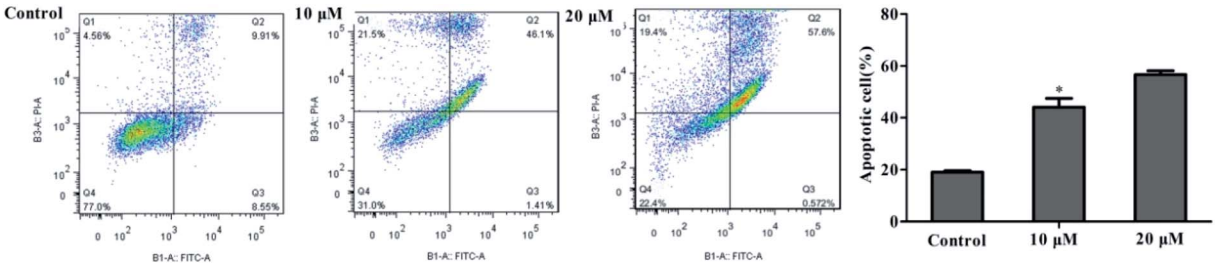

Fig. 5 Effect of **4k** on apoptosis in MCF-7 cells. Flow cytometry analyses of MCF-7 cells after Annexin V-FITC/PI staining revealed that **4k** exposure resulted in apoptosis in MCF-7 cells in a concentration-dependent manner. *$P < 0.05$ *vs.* the control group.

shown in Fig. 5, the apoptosis rate of the control group was (19.05 ± 0.83)%; however, the treatment of MCF-7 cells for 24 h in the low-concentration group (10 μM) of **4k** led to a reduction in cell viability of (46.63 ± 1.25)%. Moreover, a higher value of (57.69 ± 0.68)% was observed at a higher concentration (20 μM) of **4k**. Therefore, it is suggested that at these concentrations, **4k** could induce cell death in MCF-7 cells.

Conclusions

In this work, we synthesized 14 novel dihomooxacalix[4]arene N-heterocyclic derivatives, namely, **4a–4n**. In the subsequent cytotoxicity test, 1,3-disubstituted N-heterocyclic derivatives were found to be more effective than mono-N-heterocyclic-linked derivatives. Moreover, **4d–4f** and **4k** show significant effects at inducing cytotoxicity on all the four parental types of cancer cells, but exhibit low toxicity toward normal cells. The results of the molecular studies presented in this study revealed that **4k** could induce apoptosis, upregulate protein expression levels of Bax and cleaved caspase-3, and downregulate Bcl-2 in human breast cancer cells. Therefore, the dihomooxacalix[4]arene N-heterocyclic derivative is expected to garner a new generation of supramolecular antitumor drugs.

Experimental section

Materials and apparatus

All the reagents and solvents were commercial reagents with analytical grade. Further, *p-tert*-butyl dihomooxacalix[4]arene **1** was prepared according to the procedures in the literature.[20] Furthermore, dihomooxacalix[4]arene ester **2a–2b** and carboxylic acid **3a–3b** were similarly synthesized as described earlier.[15,16,21] The melting points were determined with capillaries with a YRT-3 microscope apparatus and were uncorrected. The ^{1}H NMR and ^{13}C NMR spectra were recorded at 400 MHz on a Bruker AV-400 spectrometer. The HRMS data were obtained using a maXis 4G (UHR-TOF) instrument. The reactions were monitored by thin-layer chromatography (TLC) using 2.5 mm Merck silica gel F254 strips. Distilled water was used in the experiments. Experimental cells were obtained from the Cell Bank, Chinese Academy of Sciences. All the reagents and kits used in the cell experiments are commercially available.

Generic procedure for the synthesis of compounds 4a–4f

Here, **2a** (0.23 g, 0.3 mmol) or **2b** (0.26 g, 0.3 mmol) was dissolved in aminomethylpyridine (2 mL) and stirred at the ambient temperature. Upon the completion of the reaction (TLC monitoring; typically, 4 h), water was added to the reaction mixture and then filtered, leaving a pale-yellow solid that was later purified by flash chromatography (silica gel/dichloromethane/methanol) to yield the product in a quantitative yield.

7,13,19,25-Tetra-*tert*-butyl-28,29,30-tri-hydroxy-27-(*N*-(2-pyridin-4-ylmethyl)-aminocarbonylmethoxyl)-2,3-dihomo-3-oxacalix[4]arene (4a). White solid, yield 90.1%, mp 155.9–157.2 °C; IR (KBr, cm^{-1}) ν 3333, 2961, 2868, 1690, 1603, 1487, 1362, 1209, 1074, 876; ^{1}H NMR ($CDCl_3$, 400 MHz) δ 9.31 (t, 1H, J = 5.6 Hz), 8.86 (s, 1H), 8.53 (dd, 2H, J = 4.4, 1.6 Hz), 8.49 (s, 1H), 7.80 (s, 1H), 7.39 (d, 2H, J = 5.6 Hz), 7.28 (t, 2H, J = 2.4 Hz), 7.16 (d, 1H, J = 2.4 Hz), 7.14–7.12 (m, 2H), 7.09 (d, 1H, J = 2.4 Hz), 6.93 (d, 1H, J = 2.4 Hz), 6.91 (d, 1H, J = 2.4 Hz), 4.97 (d, 1H, J = 15.2 Hz), 4.79 (d, 1H, J = 6.0 Hz), 4.76–4.72 (m, 1H), 4.63–4.50 (m, 3H), 4.36 (d, 1H, J = 10.2 Hz), 4.21 (d, 1H, J = 9.6 Hz), 4.17–4.03 (m, 3H), 3.60 (d, 1H, J = 13.6 Hz), 3.46 (dd, 2H, J = 18.0, 14.0 Hz), 1.26 (s, 9H), 1.23 (d, 18H, J = 1.2 Hz), 1.16 (s, 9H); ^{13}C NMR ($CDCl_3$, 100 MHz) δ 168.2, 151.7, 150.8, 150.1, 149.0, 148.5, 147.2, 146.8, 144.2, 143.0, 142.9, 132.1, 131.6, 128.2, 127.7, 127.3, 127.2, 127.1, 126.8, 126.4, 126.1, 125.8, 125.5, 124.5, 122.9, 122.2, 74.4, 71.7, 71.5, 42.4, 34.3, 34.0, 33.9, 33.8, 32.3, 31.5, 31.4, 31.1, 31.0; MS (*m*/*z*): HRMS (ESI) calcd for $C_{53}H_{67}N_2O_6$ ($[M + H]^+$): 827.4999, found: 827.5013.

7,13,19,25-Tetra-*tert*-butyl-28,29,30-tri-hydroxy-27-(*N*-(2-pyridin-3-ylmethyl)-aminocarbonylmethoxyl)-2,3-dihomo-3-oxacalix[4]arene (4b). White solid, yield 82.9%, mp 154.1–156.9 °C; IR (KBr, cm^{-1}) ν 3331, 2959, 2868, 1686, 1605, 1535, 1487, 1364, 1202, 1076, 712; ^{1}H NMR ($CDCl_3$, 400 MHz) δ 9.24 (t, 1H, J = 5.6 Hz), 8.81 (s, 1H), 8.71 (d, 1H, J = 2.0 Hz), 8.46 (dd, 1H, J = 4.8, 1.6 Hz), 8.33 (s, 1H), 7.86–7.81 (m, 1H), 7.76 (s, 1H), 7.27–7.26 (m, 2H), 7.21 (dd, 1H, J = 8.0, 4.8 Hz), 7.14 (d, 1H, J = 2.4 Hz), 7.11 (s, 2H), 7.08 (d, 1H, J = 2.4 Hz), 6.93 (d, 1H, J = 2.4 Hz), 6.90 (d, 1H, J = 2.4 Hz), 4.96 (d, 1H, J = 14.8 Hz), 4.82 (d, 1H, J = 5.2 Hz), 4.78 (d, 1H, J = 6.2 Hz), 4.62–4.59 (m, 1H), 4.61–4.51 (m, 2H), 4.37 (d, 1H, J = 10.2 Hz), 4.21 (d, 1H, J = 9.6 Hz), 4.13 (d, 1H, J = 9.0 Hz), 4.09 (d, 1H, J = 9.6 Hz), 4.02 (d, 1H, J = 13.6 Hz), 3.59 (d, 1H, J = 13.6 Hz), 3.44 (d, 1H, J = 14.0 Hz), 3.38 (d, 1H, J = 13.2 Hz), 1.26 (s, 9H), 1.22 (d, 18H, J = 2.0 Hz), 1.15 (s,

9H); ^{13}C NMR ($CDCl_3$, 100 MHz) δ 168.0, 151.7, 150.9, 149.8, 149.0, 148.9, 148.5, 147.2, 144.2, 142.9, 142.7, 136.0, 133.5, 132.1, 131.6, 128.2, 127.7, 127.4, 127.2, 127.1, 126.8, 126.4, 126.1, 125.7, 125.6, 125.5, 124.4, 123.6, 122.9, 122.2, 74.3, 71.7, 71.5, 41.0, 34.3, 34.0, 33.9, 32.3, 31.6, 31.5, 31.4, 31.1, 30.9; MS (*m*/*z*): HRMS (ESI) calcd for $C_{53}H_{67}N_2O_6$ ([M + H]$^+$): 827.4999, found: 827.5012.

7,13,19,25-Tetra-*tert*-butyl-28,29,30-tri-hydroxy-27-(*N*-(2-pyridin-2-ylmethyl)-aminocarbonylmethoxyl)-2,3-dihomo-3-oxacalix[4]arene (4c). White solid, yield 89.2%, mp 163.7–165.4 °C; IR (KBr, cm^{-1}) ν 3346, 2961, 2868, 1682, 1593, 1487, 1362, 1209, 1076, 874; ^{1}H NMR ($CDCl_3$, 400 MHz) δ 9.30 (t, 1H, J = 5.6 Hz), 8.84 (s, 1H), 8.55 (d, 1H, J = 4.0 Hz), 8.46 (s, 1H), 7.70 (s, 1H), 7.65–7.61 (m, 1H), 7.47 (d, 1H, J = 7.8 Hz), 7.30–7.24 (m, 2H), 7.16–7.10 (m, 4H), 7.08 (d, 1H, J = 2.4 Hz), 6.93 (d, 1H, J = 2.4 Hz), 6.89 (d, 1H, J = 2.4 Hz), 4.96 (dd, 2H, J = 15.2, 5.6 Hz), 4.82–4.69 (m, 2H), 4.77–4.71 (m, 2H), 4.34 (d, 1H, J = 10.0 Hz), 4.25 (s, 1H), 4.21 (d, 1H, J = 9.0 Hz), 4.17–4.06 (m, 2H), 3.59 (d, 1H, J = 13.8 Hz), 3.43 (t, 2H, J = 13.8 Hz), 1.25 (s, 9H), 1.23 (brs, 18H), 1.16 (s, 9H); ^{13}C NMR ($CDCl_3$, 100 MHz) δ 168.2, 157.5, 151.9, 151.0, 149.4, 148.8, 148.7, 147.4, 144.0, 142.7, 142.6, 136.7, 132.0, 131.8, 128.1, 127.7, 127.5, 127.2, 127.1, 126.7, 126.6, 126.0, 125.8, 125.5, 125.4, 124.4, 122.7, 122.3, 122.1, 121.5, 74.6, 71.8, 71.4, 45.0, 34.3, 34.0, 33.9, 33.8, 32.3, 31.6, 31.5, 31.4, 31.3, 31.1, 31.0; MS (*m*/*z*): HRMS (ESI) calcd for $C_{53}H_{67}N_2O_6$ ([M + H]$^+$): 827.4999, found: 827.5009.

7,13,19,25-Tetra-*tert*-butyl-28,30-di-hydroxy-27,29-di-(*N*-(2-pyridin-4-ylmethyl)-aminocarbonylmethoxyl)-2,3-dihomo-3-oxacalix[4]arene (4d). White solid, yield 93.2%, mp 129.7–130.1 °C; IR (KBr, cm^{-1}) ν 3369, 2969, 2868, 1678, 1537, 1483, 1362, 1192, 1070, 876, 714; ^{1}H NMR ($CDCl_3$, 400 MHz) δ 9.55 (dd, 1H, J = 6.4, 5.6 Hz), 9.18 (t, 1H, J = 5.2 Hz), 8.50 (d, 2H, J = 5.6 Hz), 8.33 (d, 2H, J = 5.2 Hz), 8.00 (s, 1H), 7.44 (d, 1H, J = 1.6 Hz), 7.34–7.32 (m, 3H), 7.23 (d, 3H, J = 3.2 Hz), 7.17 (d, 2H, J = 8.4 Hz), 7.13 (s, 1H), 7.01 (d, 2H, J = 8.4 Hz), 6.85 (d, 1H, J = 1.2 Hz), 4.92–4.85 (m, 2H), 4.81 (d, 1H, J = 10.0 Hz), 4.75 (d, 1H, J = 10.0 Hz), 4.69 (d, 1H, J = 15.2 Hz), 4.56 (d, 1H, J = 15.2 Hz), 4.46–4.36 (m, 3H), 4.26 (s, 2H), 4.18 (d, 1H, J = 10.4 Hz), 4.12 (t, 2H, J = 14.4 Hz), 3.94 (d, 1H, J = 13.6 Hz), 3.53 (d, 1H, J = 13.6 Hz), 3.41 (dd, 2H, J = 13.6, 6.4 Hz), 1.28 (d, 18H, J = 3.2 Hz), 1.24 (s, 9H), 1.16 (s, 9H); ^{13}C NMR ($CDCl_3$, 100 MHz) δ 31.0, 31.1, 31.2, 31.5, 32.3, 33.9, 34.2, 34.3, 42.3, 42.6, 71.2, 72.1, 73.5, 74.3, 122.2, 123.0, 124.5, 125.7, 126.0, 126.1, 126.8, 127.1, 127.2, 127.6, 128.6, 129.5, 131.4, 132.2, 133.6, 143.2, 143.8, 146.1, 146.8, 148.3, 148.8, 149.2, 149.9, 150.0, 150.9, 152.8, 168.4, 168.9; MS (*m*/*z*): HRMS (ESI) calcd for $C_{61}H_{74}N_4NaO_7$ ([M + Na]$^+$): 997.5458, found: 997.5475.

7,13,19,25-Tetra-*tert*-butyl-28,30-di-hydroxy-27,29-di-(*N*-(2-pyridin-3-ylmethyl)-aminocarbonylmethoxyl)-2,3-dihomo-3-oxacalix[4]arene (4e). White solid, yield 94.5%, mp 130.5–131.7 °C; IR (KBr, cm^{-1}) ν 3377, 2961, 2868, 1678, 1603, 1541, 1485, 1417, 1362, 1202, 1070, 876; ^{1}H NMR ($CDCl_3$, 400 MHz) δ 9.43 (t, 1H, J = 5.6 Hz), 9.14 (dd, 1H, J = 5.6, 4.8 Hz), 8.70 (d, 1H, J = 2.0 Hz), 8.63 (d, 1H, J = 2.0 Hz), 8.49 (dd, 1H, J = 4.8, 1.6 Hz), 8.37 (dd, 1H, J = 4.8, 1.6 Hz), 7.88 (s, 1H), 7.75 (dt, 1H, J = 8.0, 2.0 Hz), 7.60 (dt, 1H, J = 8.0, 2.0 Hz), 7.42 (d, 1H, J = 2.4 Hz), 7.31 (s, 1H), 7.17 (dd, 2H, J = 7.6, 5.2 Hz), 7.14 (dd, 2H, J = 4.4, 2.4 Hz), 7.11 (d, 1H, J = 2.4 Hz), 7.03 (d, 1H, J = 2.8 Hz), 6.95 (d, 1H, J = 2.8 Hz), 6.94 (d, 1H, J = 4.8 Hz), 6.84 (d, 1H, J = 2.4 Hz), 4.89–4.86 (m, 1H), 4.82 (d, 1H, J = 5.2 Hz), 4.79 (d, 1H, J = 5.2 Hz), 4.77 (d, 1H, J = 4.4 Hz), 4.72 (d, 1H, J = 15.2 Hz), 4.56 (d, 1H, J = 15.2 Hz), 4.49–4.40 (m, 4H), 4.28 (d, 1H, J = 10.0 Hz), 4.20 (d, 1H, J = 10.4 Hz), 4.10 (d, 1H, J = 13.2 Hz), 4.03 (d, 1H, J = 13.2 Hz), 3.97 (d, 1H, J = 13.2 Hz), 3.49 (d, 1H, J = 13.6 Hz), 3.38 (dd, 2H, J = 13.2, 3.6 Hz), 1.27 (d, 18H, J = 2.8 Hz), 1.24 (s, 9H), 1.15 (s, 9H); ^{13}C NMR ($CDCl_3$, 100 MHz) δ 31.1, 31.2, 31.4, 31.5, 32.2, 33.8, 33.9, 34.2, 34.3, 40.9, 41.0, 71.1, 72.2, 73.7, 122.2, 123.3, 123.4, 124.5, 125.8, 126.2, 126.7, 126.8, 127.0, 127.1, 127.2, 127.6, 128.6, 129.4, 131.4, 132.2, 133.2, 133.6, 133.7, 135.8, 136.0, 143.0, 143.6, 148.2, 148.3, 148.6, 148.7, 148.9, 149.5, 149.6, 149.7, 151.0, 152.8, 168.2, 168.7; MS (*m*/*z*): HRMS (ESI) calcd for $C_{61}H_{74}N_4NaO_7$ ([M + Na]$^+$): 997.5558, found: 997.5474.

7,13,19,25-Tetra-*tert*-butyl-28,30-di-hydroxy-27,29-di-(*N*-(2-pyridin-2-ylmethyl)-aminocarbonylmethoxyl)-2,3-dihomo-3-oxacalix[4]arene (4f). White solid, yield 91.8%, mp 131.3–132.2 °C; IR (KBr, cm^{-1}) ν 3381, 2961, 2868, 1678, 1535, 1483, 1362, 1192, 1070, 874, 754; ^{1}H NMR ($CDCl_3$, 400 MHz) δ 9.22 (t, 1H, J = 5.6 Hz), 8.97 (t, 1H, J = 5.6 Hz), 8.38 (d, 1H, J = 4.4 Hz), 8.21 (d, 1H, J = 4.4 Hz), 7.80 (s, 1H), 7.55–7.47 (m, 2H), 7.40 (d, 1H, J = 2.4 Hz), 7.38 (d, 1H, J = 8.0 Hz), 7.31 (d, 1H, J = 8.0 Hz), 7.17 (s, 2H), 7.13 (d, 1H, J = 2.0 Hz), 7.06 (t, 2H, J = 2.0 Hz), 7.04–7.01 (m, 1H), 7.00 (d, 1H, J = 2.4 Hz), 6.96 (dd, 1H, J = 6.8, 5.2 Hz), 6.89 (d, 1H, J = 2.0 Hz), 6.81 (d, 1H, J = 2.4 Hz), 4.89–4.81 (m, 3H), 4.69–4.62 (m, 4H), 4.59–4.50 (m, 4H), 4.28 (dd, 2H, J = 14.8, 10.4 Hz), 4.20 (d, 1H, J = 5.6 Hz), 4.17 (d, 1H, J = 9.2 Hz), 4.10 (d, 1H, J = 13.2 Hz), 3.44 (d, 1H, J = 13.6 Hz), 3.35 (t, 2H, J = 14.4 Hz), 1.25 (d, 18H, J = 2.0 Hz), 1.22 (s, 9H), 1.09 (s, 9H); ^{13}C NMR ($CDCl_3$, 100 MHz) δ 31.0, 31.2, 31.3, 31.4, 31.5, 31.6, 32.2, 33.8, 33.9, 34.2, 44.8, 45.0, 71.1, 72.4, 73.7, 74.5, 121.9, 122.0, 122.1, 122.3, 124.2, 125.5, 125.6, 125.9, 126.5, 126.8, 126.9, 127.2, 127.6, 127.7, 128.8, 129.4, 131.9, 132.0, 133.9, 136.3, 136.4, 142.3, 143.0, 147.8, 148.1, 149.0, 149.1, 149.2, 150.0, 151.7, 153.1, 157.0, 157.6, 168.4, 168.9; MS (*m*/*z*): HRMS (ESI) calcd for $C_{61}H_{74}N_4NaO_7$ ([M + Na]$^+$): 997.5558, found: 997.5470.

Generic procedure for the synthesis of compound 4g–4n

A mixture of carboxylic acid **3a** or **3b** (0.22 g or 0.25 g, 0.3 mmol) and oxalyl chloride (0.75 g, 5.9 mmol) was dissolved in dry dichloromethane (2 mL) and stirred at room temperature. After 5 h, the mixture was evaporated and washed with dichloromethane 3 times to afford the solid. To a solution of the above solid in dry dichloromethane (4 mL), 1.2 mmol of amino-substituted pyridine (or quinoline or thiazole) was slowly added dropwise in 2 mL of THF at 0 °C. The reaction was completed after 6–12 h. The evaporation of the solvent yielded the crude products, which were subsequently subjected to flash chromatography to afford **4g–4n**.

7,13,19,25-Tetra-*tert*-butyl-28,29,30-tri-hydroxy-27-(*N*-(6-quinolyl)-aminocarbonylmethoxyl)-2,3-dihomo-3-oxacalix[4]arene (4g). White solid, yield 92.4%, mp 179.2–180.6 °C; IR (KBr) ν 3367, 2961, 2868, 1701, 1545, 1487, 1383, 1364, 1209, 875; ^{1}H NMR ($CDCl_3$, 400 MHz) δ 10.65 (s, 1H), 8.99 (s, 1H),

8.86–8.81 (m, 2H), 8.61 (d, 1H, J = 2.2 Hz), 8.29 (s, 1H), 8.25 (dd, 1H, J = 2.4 Hz), 8.20–8.15 (m, 1H), 8.10 (d, 1H, J = 9.2 Hz), 7.38 (dd, 2H, J = 8.4, 4.2 Hz), 7.31 (d, 1H, J = 2.4 Hz), 7.29 (d, 1H, J = 2.4 Hz), 7.19 (d, 1H, J = 2.4 Hz), 7.16 (s, 2H), 7.12 (d, 1H, J = 2.4 Hz), 7.01 (d, 1H, J = 2.4 Hz), 6.93 (d, 1H, J = 2.4 Hz), 5.08 (d, 1H, J = 5.4 Hz), 5.05 (s, 1H), 4.77 (d, 1H, J = 10.2 Hz), 4.68 (d, 1H, J = 15.2 Hz), 4.51 (d, 1H, J = 10.2 Hz), 4.37 (d, 1H, J = 9.6 Hz), 4.25 (d, 1H, J = 1.5 Hz), 4.21 (d, 1H, J = 2.8 Hz), 4.11 (d, 1H, J = 13.8 Hz), 3.66 (d, 1H, J = 13.8 Hz), 3.50 (d, 1H, J = 7.2 Hz), 3.46 (d, 1H, J = 6.4 Hz), 1.24 (d, 27H, J = 1.0 Hz), 1.17 (s, 9H); ^{13}C NMR ($CDCl_3$, 100 MHz) δ 166.5, 151.9, 151.1, 151.0, 149.5, 149.2, 148.6, 147.3, 145.8, 144.5, 144.4, 143.1, 143.0, 136.2, 135.9, 135.8, 132.1, 131.6, 130.0, 128.8, 128.5, 127.7, 127.5, 127.4, 127.3, 126.9, 126.5, 126.3, 125.9, 125.8, 125.6, 124.4, 124.2, 122.8, 122.3, 121.6, 117.2, 74.6, 72.1, 71.9, 34.4, 34.1, 34.0, 32.5, 31.6, 31.5, 31.2; MS (m/z): HRMS (ESI) calcd for $C_{56}H_{67}N_2O_6$ ([M + H]$^+$): 863.4999, found: 863.4991.

7,13,19,25-Tetra-*tert*-butyl-28,29,30-tri-hydroxy-27-(*N*-(3-quinolyl)-aminocarbonylmethoxyl)-2,3-dihomo-3-oxacalix[4]arene (4h). White solid, yield 93.9%, mp 188.7–189.2 °C; IR (KBr, cm^{-1}) ν 3331, 2961, 2905, 2868, 1697, 1545, 1487, 1382, 1209, 876; ^{1}H NMR ($CDCl_3$, 400 MHz) δ 10.77 (s, 1H), 9.37 (d, 1H, J = 2.4 Hz), 8.98 (d, 2H, J = 2.4 Hz), 8.77 (s, 1H), 8.28 (s, 1H), 8.08 (dd, 1H, J = 8.4, 0.8 Hz), 7.85 (dd, 1H, J = 8.2, 1.2 Hz), 7.66–7.61 (m, 1H), 7.56–7.51 (m, 1H), 7.29 (s, 1H), 7.28 (s, 1H), 7.19 (d, 1H, J = 2.4 Hz), 7.15 (d, 2H, J = 2.4 Hz), 7.12 (d, 1H, J = 2.4 Hz), 6.99 (d, 1H, J = 2.4 Hz), 6.93 (d, 1H, J = 2.4 Hz), 5.11 (d, 1H, J = 3.0 Hz), 5.08 (d, 1H, J = 8.8 Hz), 4.85 (d, 1H, J = 10.2 Hz), 4.71 (d, 1H, J = 15.2 Hz), 4.49 (d, 1H, J = 10.4 Hz), 4.34 (d, 1H, J = 9.6 Hz), 4.24 (d, 1H, J = 7.2 Hz), 4.21 (d, 1H, J = 8.2 Hz), 4.11 (d, 1H, J = 13.6 Hz), 3.65 (d, 1H, J = 14.0 Hz), 3.49 (d, 1H, J = 4.0 Hz), 3.46 (d, 1H, J = 4.8 Hz), 1.24, 1.17 (2s, 36H); ^{13}C NMR ($CDCl_3$, 100 MHz) δ 167.0, 151.8, 151.0, 149.3, 148.6, 147.3, 145.6, 145.0, 144.5, 143.3, 143.0, 132.2, 131.7, 131.6, 129.2, 128.5, 128.4, 128.3, 128.0, 127.7, 127.5, 127.4, 127.2, 127.0, 126.5, 126.3, 126.0, 125.8, 125.6, 124.7, 124.6, 123.1, 122.4, 74.6, 72.1, 71.9, 34.4, 34.1, 34.0, 32.5, 31.7, 31.6, 31.5, 31.4, 31.2; MS (m/z): HRMS (ESI) calcd for $C_{56}H_{67}N_2O_6$ ([M + H]$^+$): 863.4999, found: 863.5004.

7,13,19,25-Tetra-*tert*-butyl-28,30-di-hydroxy-27,29-di-(*N*-(8-quinolyl)-aminocarbonylmethoxyl)-2,3-dihomo-3-oxacalix[4]arene (4i). White solid, yield 85.4%, mp 157.3–158.5 °C; IR (KBr, cm^{-1}) ν 3435, 2960, 2906, 1686, 1535, 1485, 1194, 874; ^{1}H NMR ($CDCl_3$, 400 MHz) δ 10.74 (s, 2H), 8.54 (d, 1H, J = 3.0 Hz), 8.49–8.41 (m, 3H), 7.32–7.26 (m, 6H), 7.17 (s, 2H), 7.09 (s, 2H), 7.00 (d, 2H, J = 2.4 Hz), 6.90 (d, 1H, J = 1.2 Hz), 6.85 (d, 1H, J = 2.4 Hz), 6.75 (d, 1H, J = 1.2 Hz), 5.02 (d, 1H, J = 10.2 Hz), 4.80 (s, 2H), 4.69 (s, 2H), 4.60–4.33 (m, 5H), 4.29 (d, 1H, J = 10.6 Hz), 3.55 (d, 2H, J = 15.0 Hz), 3.46 (d, 1H, J = 15.0 Hz), 1.30, 1.25, 1.09, 0.95 (4s, 36H); ^{13}C NMR ($CDCl_3$, 100 MHz) δ 166.5, 152.7, 152.5, 150.4, 150.3, 148.6, 147.6, 147.3, 142.3, 141.4, 134.9, 133.6, 133.4, 133.1, 130.9, 128.7, 127.9, 127.6, 127.4, 127.3, 126.5, 126.4, 126.3, 126.0, 125.9, 125.3, 123.9, 122.8, 122.1, 121.5, 121.3, 116.8, 74.3, 73.8, 34.2, 34.1, 34.0, 33.9, 31.8, 31.7, 31.3, 31.2; MS (m/z): HRMS (ESI) calcd for $C_{67}H_{75}N_4O_7$ ([M + H]$^+$): 1047.5636, found: 1047.5656.

7,13,19,25-Tetra-*tert*-butyl-28,30-di-hydroxy-27,29-di-(*N*-(5-quinolyl)-aminocarbonylmethoxyl)-2,3-dihomo-3-oxacalix[4]arene (4j). White solid, yield 82.6%, mp 167.9–169.5 °C; IR (KBr, cm^{-1}) ν 3404, 2969, 2868, 1680, 1535, 1485, 1363, 1199, 801; ^{1}H NMR ($CDCl_3$, 400 MHz) δ 10.10 (s, 1H), 9.40 (s, 1H), 8.82 (dd, 1H, J = 4.2, 1.6 Hz), 8.69 (dd, 1H, J = 4.2, 1.6 Hz), 8.22 (d, 1H, J = 8.4 Hz), 8.12 (d, 1H, J = 8.4 Hz), 7.90–7.74 (m, 3H), 7.58–7.51 (m, 2H), 7.45 (dd, 2H, J = 10.0, 5.2 Hz), 7.40 (s, 1H), 7.32 (d, 1H, J = 2.4 Hz), 7.30–7.27 (m, 1H), 7.20 (d, 1H, J = 2.4 Hz), 7.15 (d, 1H, J = 2.4 Hz), 7.06 (dt, 3H, J = 8.6, 4.2 Hz), 6.89 (d, 1H, J = 2.4 Hz), 6.85 (d, 1H, J = 2.4 Hz), 6.82 (dd, 1H, J = 8.4, 4.2 Hz), 5.03 (d, 1H, J = 10.8 Hz), 4.69 (d, 1H, J = 15.4 Hz), 4.58 (d, 1H, J = 15.4 Hz), 4.53–4.42 (m, 4H), 4.35 (d, 1H, J = 15.4 Hz), 4.25 (d, 1H, J = 11.0 Hz), 4.20 (d, 1H, J = 3.6 Hz), 4.17 (d, 1H, J = 3.2 Hz), 3.56 (t, 2H, J = 13.6 Hz), 3.37 (d, 1H, J = 13.8 Hz), 1.31, 1.27, 1.24, 1.06 (4s, 36H); ^{13}C NMR ($CDCl_3$, 100 MHz) δ 167.4, 166.5, 152.5, 151.5, 150.2, 150.1, 149.1, 148.6, 148.3, 148.2, 142.8, 132.4, 131.3, 131.0, 129.8, 129.7, 129.3, 128.8, 128.0, 127.8, 127.6, 127.5, 127.3, 127.1, 126.8, 126.3, 126.0, 125.9, 124.1, 122.1, 120.7, 120.5, 120.3, 74.2, 73.9, 72.0, 71.1, 34.3, 34.2, 34.0, 33.9, 32.8, 31.6, 31.5, 31.2, 31.0, 30.8; MS (m/z): HRMS (ESI) calcd for $C_{67}H_{75}N_4O_7$ ([M + H]$^+$): 1047.5636, found: 1047.5640.

7,13,19,25-Tetra-*tert*-butyl-28,30-di-hydroxy-27,29-di-(*N*-(3-quinolyl)-aminocarbonylmethoxyl)-2,3-dihomo-3-oxacalix[4]arene (4k). White solid, yield 88.7%, mp 156.4–157.9 °C; IR (KBr, cm^{-1}) ν 3400, 2961, 2868, 1699, 1545, 1485, 1364, 1194, 876; ^{1}H NMR ($CDCl_3$, 400 MHz) δ 10.68 (s, 1H), 10.49 (s, 1H), 9.10 (d, 1H, J = 2.6 Hz), 8.93 (d, 1H, J = 2.6 Hz), 8.58 (s, 1H), 8.19–8.17 (m, 1H), 8.11 (dd, 1H, J = 8.4, 0.8 Hz), 8.09–8.05 (m, 3H), 7.69–7.63 (m, 2H), 7.56 (d, 1H, J = 1.0 Hz), 7.55 (d, 1H, J = 0.8 Hz), 7.52 (dd, 2H, J = 7.6, 1.6 Hz), 7.48 (dd, 1H, J = 8.2, 1.4 Hz), 7.30 (d, 1H, J = 2.4 Hz), 7.21 (t, 2H, J = 2.4 Hz), 7.19 (d, 1H, J = 2.4 Hz), 7.09 (d, 1H, J = 2.4 Hz), 7.06 (d, 1H, J = 2.4 Hz), 6.87 (d, 1H, J = 2.4 Hz), 5.29 (d, 1H, J = 10.8 Hz), 5.03 (d, 1H, J = 15.2 Hz), 4.92 (d, 1H, J = 15.2 Hz), 4.80 (d, 1H, J = 10.6 Hz), 4.60 (d, 1H, J = 10.6 Hz), 4.46 (d, 1H, J = 12.8 Hz), 4.38 (s, 1H), 4.34 (d, 1H, J = 8.4 Hz), 4.29 (d, 1H, J = 1.6 Hz), 4.25 (d, 1H, J = 8.6 Hz), 4.20 (d, 1H, J = 4.8 Hz), 4.17 (d, 1H, J = 2.8 Hz), 3.74 (d, 1H, J = 14.0 Hz), 3.47 (d, 1H, J = 12.8 Hz), 3.42 (d, 1H, J = 13.2 Hz), 1.30, 1.26, 1.22, 1.18 (4s, 36H); ^{13}C NMR ($CDCl_3$, 100 MHz) δ 167.0, 165.8, 153.1, 151.3, 149.2, 149.0, 148.9, 148.1, 145.5, 143.5, 143.4, 143.2, 133.6, 132.2, 131.7, 131.3, 130.0, 128.4, 128.1, 127.9, 127.6, 127.5, 127.1, 126.5, 124.5, 123.8, 123.6, 122.3, 74.2, 73.8, 71.5, 34.5, 31.7, 31.6, 31.4, 31.3; MS (m/z): HRMS (ESI) calcd for $C_{67}H_{75}N_4O_7$ ([M + H]$^+$): 1047.5636, found: 1047.5641.

7,13,19,25-Tetra-*tert*-butyl-28,30-di-hydroxy-27,29-di-(*N*-(2-thiazolyl)-aminocarbonylmethoxyl)-2,3-dihomo-3-oxacalix[4]arene (4l). White solid, yield 93.2%, mp 163.5–165.1 °C; IR (KBr, cm^{-1}) ν 3367, 3325, 2980, 2871, 1598, 1535, 1481, 1333, 1193, 875; ^{1}H NMR ($CDCl_3$, 400 MHz) δ 12.30 (s, 1H), 12.00 (s, 1H), 8.81 (s, 1H), 8.17 (s, 1H), 7.50 (d, 1H, J = 2.4 Hz), 7.44 (d, 1H, J = 3.5 Hz), 7.42 (d, 1H, J = 3.5 Hz), 7.24–7.21 (m, 2H), 7.20 (d, 1H, J = 2.4 Hz), 7.15 (d, 1H, J = 2.3 Hz), 7.09 (dd, 2H, J = 4.4, 2.4 Hz), 6.86 (q, 3H, J = 3.2 Hz), 5.20 (d, 1H, J = 15.6 Hz), 5.14 (s, 1H), 5.11 (d, 1H, J = 4.4 Hz), 4.72 (d, 1H, J = 10.0 Hz), 4.56 (d, 1H, J = 15.4 Hz), 4.46 (d, 1H, J = 5.4 Hz), 4.43 (d, 1H, J = 10.8

Hz), 4.37 (d, 1H, J = 13.0 Hz), 4.31 (d, 1H, J = 10.4 Hz), 4.26 (d, 1H, J = 13.8 Hz), 4.17 (d, 1H, J = 13.1 Hz), 3.65 (d, 1H, J = 13.8 Hz), 3.45 (d, 1H, J = 8.8 Hz), 3.42 (d, 1H, J = 8.8 Hz), 1.27 (d, 18H, J = 1.6 Hz), 1.23, 1.19 (2s, 18H); ^{13}C NMR ($CDCl_3$, 100 MHz) δ 166.8, 166.3, 157.1, 156.7, 153.1, 151.9, 149.5, 149.3, 148.5, 147.9, 143.1, 142.6, 138.1, 137.9, 133.8, 132.3, 131.6, 129.7, 129.2, 127.4, 127.3, 127.2, 126.5, 126.0, 125.9, 125.5, 124.0, 122.2, 113.4, 113.3, 74.0, 73.3, 72.1, 71.2, 34.5, 34.3, 33.9, 32.8, 31.8, 31.6, 31.2, 31.1; MS (m/z): HRMS (ESI) calcd for $C_{55}H_{66}N_4NaO_7S_2$ ([M + Na]$^+$): 981.4271, found: 981.4281.

7,13,19,25-Tetra-*tert*-butyl-28,30-di-hydroxy-27,29-di-(*N*-(4-pyridyl)-aminocarbonylmethoxyl)-2,3-dihomo-3-oxacalix[4]arene (4m). White solid, yield 89.2%, mp 166.8–168.5 °C; IR (KBr, cm^{-1}) ν 3392, 3378, 2980, 2867, 1699, 1591, 1483, 1207, 1193, 825; ^{1}H NMR ($CDCl_3$, 400 MHz) δ 10.54 (s, 1H), 10.31 (s, 1H), 8.51 (s, 1H), 8.48 (t, 4H, J = 5.6 Hz), 7.92 (s, 1H), 7.50 (t, 3H, J = 2.4 Hz), 7.44 (d, 2H, J = 6.4 Hz), 7.32 (d, 1H, J = 2.4 Hz), 7.24 (d, 1H, J = 2.4 Hz), 7.21 (dd, 2H, J = 4.0, 2.4 Hz), 7.09 (t, 2H, J = 2.4 Hz), 6.88 (d, 1H, J = 2.4 Hz), 5.14 (s, 1H), 4.91 (d, 1H, J = 15.6 Hz), 4.81 (d, 1H, J = 15.2 Hz), 4.64 (d, 1H, J = 10.4 Hz), 4.58 (d, 1H, J = 10.8 Hz), 4.39 (s, 1H), 4.35 (d, 1H, J = 3.6 Hz), 4.29 (d, 1H, J = 11.2 Hz), 4.20 (d, 1H, J = 15.2 Hz), 4.14 (d, 1H, J = 14.0 Hz), 4.09 (d, 1H, J = 13.2 Hz), 3.75 (d, 1H, J = 13.6 Hz), 3.47 (d, 1H, J = 12.8 Hz), 3.42 (d, 1H, J = 13.2 Hz), 1.30, 1.27, 1.24, 1.19 (4s, 36H); ^{13}C NMR ($CDCl_3$, 100 MHz) δ 167.2, 166.1, 153.0, 151.1, 150.6, 149.3, 149.0, 148.8, 148.3, 144.6, 144.4, 144.3, 143.6, 133.5, 132.1, 131.6, 128.6, 127.6, 127.7, 127.6, 127.5, 126.4, 126.0, 125.9, 122.0, 113.8, 113.5, 74.1, 73.7, 72.1, 71.5, 34.5, 34.4, 34.2, 34.1, 31.7, 31.6, 31.4, 31.2; MS (m/z): HRMS (ESI) calcd for $C_{59}H_{71}N_4O_7$ ([M + H]$^+$): 947.5323, found: 947.5342.

7,13,19,25-Tetra-*tert*-butyl-28,30-di-hydroxy-27,29-di-(*N*-(2-pyridyl)-aminocarbonylmethoxyl)-2,3-dihomo-3-oxacalix[4]arene (4n). White solid, yield 93.6%, mp 160.5–162.2 °C; IR (KBr, cm^{-1}) ν 3367, 3325, 2980, 2871, 1598, 1535, 1481, 1333, 1193, 875; ^{1}H NMR ($CDCl_3$, 400 MHz) δ 11.02 (s, 1H), 10.96 (s, 1H), 8.61 (s, 1H), 8.33 (s, 2H), 8.21 (s, 1H), 7.77 (d, 1H, J = 8.2 Hz), 7.67 (d, 1H, J = 8.2 Hz), 7.48 (q, 2H, J = 9.4 Hz), 7.22 (d, 2H, J = 5.6 Hz), 7.19 (s, 1H), 7.15 (s, 1H), 7.08 (s, 2H), 7.03–6.94 (m, 2H), 6.83 (s, 1H), 5.15 (d, 1H, J = 10.6 Hz), 4.96 (d, 1H, J = 15.4 Hz), 4.85 (d, 1H, J = 15.2 Hz), 4.57 (d, 1H, J = 10.2 Hz), 4.50–4.42 (m, 2H), 4.42–4.31 (m, 2H), 4.31–4.27 (m, 2H), 4.24 (d, 1H, J = 6.4 Hz), 3.63 (d, 1H, J = 13.8 Hz), 3.41 (d, 2H, J = 13.0 Hz), 1.27, 1.26, 1.22, 1.19 (4s, 36H); ^{13}C NMR ($CDCl_3$, 100 MHz) δ 167.5, 166.9, 152.2, 151.2, 149.9, 149.8, 148.1, 147.8, 147.7, 147.5, 137.5, 133.8, 132.3, 131.8, 129.7, 129.0, 127.5, 127.1, 126.7, 125.9, 123.7, 122.1, 119.7, 114.4, 113.7, 74.5, 71.7, 34.3, 34.2, 33.9, 33.8, 32.7, 31.6, 31.5, 31.3, 31.2; MS (m/z): HRMS (ESI) calcd for $C_{59}H_{71}N_4O_7$ ([M + H]$^+$): 947.5323, found: 947.5310.

Crystallography

The single crystal of compound **4f** was formed in ethanol. The single-crystal structure was determined on a Bruker Smart Apex single-crystal diffractometer. All the nonhydrogen atoms were refined with anisotropic displacement parameters. The structure was solved by direct methods (SHELX-86) followed by Fourier-difference synthesis and refined by full-matrix least squares on F^2 with SHELXS-97.[22]

Cell culture

The MCF-7, HeLa, HepG2, SKOV3, and HUVEC cell lines used in this study were kindly provided by the Cell Bank of the Chinese Academy of Sciences. All the cells were cultured at 37 °C in 5% CO_2. The MCF-7 cell lines were cultured in a flask with RPMI 1640 medium containing 2 mM L-glutamine, 1.5 g L^{-1} sodium bicarbonate, 4.5 g L^{-1} glucose, 10 mM HEPES, 1.0 mM sodium pyruvate, and 10% fetal bovine serum. Other human cell lines were also cultured using 10% fetal bovine serum and 1% penicillin/streptomycin in RPMI 1640 as described earlier.[8a]

Cytotoxicity by MTT assay

The cells were cultured in a logarithmic growth phase in a culture medium containing 10% fetal bovine serum and seeded in a 96-well culture plate containing 200 μL per well. The cells were preincubated for 24 h at 37 °C in a 5% CO_2 incubator. The cells were treated with different concentrations (0, 1.25, 2.5, 5, 10, and 20 μM) of dihomooxacalix[4]arene N-heterocyclic derivatives dissolved in DMSO for 72 h. The cell viability was analyzed by the MTT reduction assay as described below. Further, 20 μL of the MTT solution (concentration: 5 mg mL^{-1}) was added to each well, and the cells were further cultured for 4 h in a 5% CO_2 incubator for the color reaction. Then, the medium was carefully discarded from each well; thereafter, 100 μL DMSO was added to each well, shaken well in the dark, and dissolved in the oven for 30 min such that the crystals were fully dissolved and evenly mixed. The OD value of each well was measured by a microplate reader at a wavelength of 550 nm. The inhibition rate of cell proliferation was determined according to the following formula:

$$\text{Inhibition rate (\%)} = (\text{control group OD value} - \text{medication group OD value})/\text{control group OD value} \times 100\%$$

The compound was then processed using GraphPad Prism 5 software to calculate the IC_{50} value of the compound.

Western blotting assay

MCF-7 cells were extracted with a cell lysis buffer. The total protein concentration was measured by the BCA method and then adjusted so that the different samples had equal concentrations. Protein was separated on a 12% sodium dodecyl sulfate-polyacrylamide gel and transferred to a polyvinylidene fluoride (PVDF) membrane. The PVDF membrane was incubated with the primary antibody overnight at 4 °C and then incubated with the secondary antibody for 2 h. The target band was scanned with Odyssey, and the results were scanned by a gel imaging system. Gray value analysis was performed using the ImageJ software.

Immunofluorescence assay

Dihomooxacalix[4]arene N-heterocyclic derivative **4k** was applied to the cells for drug-induced induction at concentrations of 0, 10, and 20 μM. After 24 h of administration, the cells

were fixed with 4% paraformaldehyde (diluted in PBS) for 15 min at room temperature. Subsequently, 0.5% Triton X-100 (diluted with PBS) was added for 30 min. An additional 5% BSA blocking solution was added and blocked at room temperature for 30 min. Then, the designated primary antibody was incubated overnight at 4 °C and then incubated with the second antibody at 37 °C for 1 h. Then, DAPI was stained in the dark for 5 min. The images were observed and collected under a confocal microscope or fluorescence microscope.

Flow cytometry assay

MCF-7 cells were seeded in 6-well plates at a density of 2×10^5 cells per well in a DMEM medium (containing 10% fetal bovine serum) and cultured at 37 °C in a 5% CO_2 incubator until the cells were attached. The cells were collected by incubating different concentrations of **4k** (0, 10, and 20 μM) with the cells for 24 h. The cells were resuspended in 500 μL binding buffer, followed by the addition of 5 μL Annexin V-FITC and 5 μL of PI. The reaction mixture was allowed to stand at room temperature for 15 min. The stained cells were analyzed by flow cytometry, and the results were analyzed using the FlowJo 7.6.1 software.

Conflicts of interest

The authors declare no conflict of interest.

Acknowledgements

This work was financially supported by the National Natural Science Foundation of China (No. 81202490). We also appreciate for technical supporting and assistance from Dr C. G Yan and Y. J. Song.

References

1 F. Bray, J. Ferlay, I. Soerjomataram, R. L. S iegel, L. A. Torre and A. J. C. Jemal, *Ca-Cancer J. Clin.*, 2018, **68**, 394–424.

2 (*a*) D. Shi, F. Khan and R. Abagyan, *J. Chem. Inf. Model.*, 2019, **59**(6), 3006–3017; (*b*) Y. C. Wu, L. Cao, W. J. Mei, H. Q. Wu, S. H. Luo, H. Y. Zhan and Z. Y. Wang, *Chem. Biol. Drug Des.*, 2018, **92**, 1232–1240; (*c*) C. Li, D. Yang, X. Cao, F. Wang, H. Jiang, H. Guo, L. Du, Q. Guo and X. Yin, *Biochem. Pharmacol.*, 2016, **113**, 57–69; (*d*) N. Widmer, C. Bardin, E. Chatelut, A. Paci, J. Beijnen, D. Levêque, G. Veal and A. Astier, *Eur. J. Cancer*, 2014, **50**, 2020–2036; (*e*) A. Levina, A. Mitra and P. A. Lay, *Metallomics*, 2009, **1**, 458–470; (*f*) H. L. Wong, R. Bendayan, A. M. Rauth, Y. Li and X. Y. Wu, *Adv. Drug Delivery Rev.*, 2007, **59**, 491–504; (*g*) C. Isanbor and D. O'Hagan, *J. Fluorine Chem.*, 2006, **127**, 303–319; (*h*) P. Nygren and R. Larsson, *J. Intern. Med.*, 2003, **253**, 46–75.

3 (*a*) Z. Livshits, R. B. Rao and S. W. Smith, *Emerg. Med. Clin. N. Am.*, 2014, **32**, 167–203; (*b*) M. O. Palumbo, P. Kavan, W. H. Miller Jr, L. Panasci, S. Assouline, N. Johnson, V. Cohen, F. Patenaude, M. Pollak, R. T. Jagoe and G. Batist, *Front. Pharmacol.*, 2013, **4**, 57; (*c*) V. T. DeVita and E. Chu, *Cancer Res.*, 2008, **68**, 8643–8653; (*d*) K. S. Brown, *Semin. Interv. Radiol.*, 2006, **23**, 99–108; (*e*) T. Connors, *Oncologist*, 1996, **1**, 180–181.

4 Y. Ohhara and H. Akita, *Jpn. J. Clin. Med.*, 2015, **73**, 133–138.

5 (*a*) J. Zhou, G. Yu and F. Huang, *Chem. Soc. Rev.*, 2017, **46**, 7021–7053; (*b*) H. Cui and B. Xu, *Chem. Soc. Rev.*, 2017, **46**, 6430–6432; (*c*) A. G. Cheetham, P. Zhang, Y. A. Lin, L. L. Lock and H. Cui, *J. Am. Chem. Soc.*, 2013, **135**, 2907–2910; (*d*) C. Zhou, L. Gan, Y. Zhang, F. Zhang, G. Wang, L. Jin and R. Geng, *Sci. China, Ser. B: Chem.*, 2009, **52**, 415–458.

6 C. D. Gutsche, B. Dhawan, K. H. No and R. Muthukrishnan, *J. Am. Chem. Soc.*, 1981, **103**, 3782–3792.

7 A. Yousaf, S. A. Hamid, N. M. Bunnori and A. A. Ishola, *Drug Des., Dev. Ther.*, 2015, **9**, 2831–2838.

8 (*a*) L. An, J. W. Wang, J. D. Liu, Z. M. Zhao and Y. J. Song, *Front. Chem.*, 2019, **7**, 732; (*b*) A. M. Hussain, M. U. Ashraf, G. Muhammad, M. N. Tahir and S. N. A. Bukhari, *Curr. Pharm. Des.*, 2017, **23**, 2377–2388; (*c*) S. Karakurt, T. F. Kellici, T. Mavromoustakos, A. G. Tzakos and M. Yilmaz, *Curr. Org. Chem.*, 2016, **20**, 1043–1057; (*d*) L. An, L. L. Han, Y. G. Zheng, X. N. Peng, Y. S. Xue, X. K. Gu, J. Sun and C. G. Yan, *Eur. J. Med. Chem.*, 2016, **123**, 21–30; (*e*) Y. Zhou, H. Li and Y. W. Yang, *Chin. Chem. Lett.*, 2015, **26**, 825–828; (*f*) S. B. Nimse and T. Kim, *Chem. Soc. Rev.*, 2013, **42**, 366–386; (*g*) F. Sansone, L. Baldini, A. Casnati and R. Ungaro, *New J. Chem.*, 2010, **34**, 2715–2728.

9 (*a*) K. Chojnackia, P. Wińskaa, M. Wielechowskaa, E. Łukowska-Chojnackaa, C. Tölzerb, K. Niefindb and M. Bretnera, *Bioorg. Chem.*, 2018, **80**, 266–275; (*b*) N. C. Desai, D. Pandya and D. Vaja, *Med. Chem. Res.*, 2017, **27**, 1–9; (*c*) J. Akhtar, A. A. Khan, Z. Ali, R. Haider and M. S. Yar, *Eur. J. Med. Chem.*, 2016, **125**, 143–189; (*d*) E. Łukowska-Chojnacka, M. Wielechowska, M. Poprzeczko and M. Bretner, *Bioorg. Med. Chem.*, 2016, **24**, 735–741; (*e*) O. Afzal, S. Kumar, M. R. Haider, M. R. Ali, R. Kumar, M. Jaggi and S. Bawa, *Eur. J. Med. Chem.*, 2015, **97**, 871–910; (*f*) P. G. Baraldi, R. Romagnoli, I. Beria, P. Cozzi, C. Geroni, N. Mongelli, N. Bianchi, C. Mischiati and R. Gambari, *J. Med. Chem.*, 2000, **43**, 2675–2684.

10 (*a*) R. F. George, S. S. Panda, E. S. M. Shalaby, A. M. Srour, I. S. A. Faragc and A. S. Girgis, *RSC Adv.*, 2016, **6**, 45434–45451; (*b*) A. Malki, M. Mohsen, H. Aziz, O. Rizk, O. Shaban, M. El-Sayed, Z. A. Sherif and H. Ashour, *Molecules*, 2016, **21**, 230–255; (*c*) K. Li, Y. Li, D. Zhou, Y. B. Fan, H. Y. Guo, T. Y. Ma, J. C. Wen, D. Liu and L. X. Zhao, *Bioorg. Med. Chem.*, 2016, **24**, 1889–1897; (*d*) Y. T. Han, G. I. Choi, D. Son, N. J. Kim, H. Yun, S. Lee, D. J. Chang, H. Hong, H. Kim, H. Ha, Y. Kim, H. Park, J. Lee and Y. Suh, *J. Med. Chem.*, 2012, **55**, 9120–9135; (*e*) V. R. Solomon and H. Lee, *Curr. Med. Chem.*, 2011, **18**, 1488–1508; (*f*) K. Matsuno, Y. Masuda, Y. Uehara, H. Sato, A. Muroya, O. Takahashi, T. Yokotagawa, T. Furuya, T. Okawara, M. Otsuka, N. Ogo, T. Ashizawa, C. Oshita, S. Tai, H. Ishii, Y. Akiyama and A. Asai, *ACS Med. Chem. Lett.*, 2010, **1**, 371–375; (*g*) V. R. Solomon, C. Hu and H. Lee, *Bioorg. Med. Chem.*, 2009, **17**, 7585–7592; (*h*)

A. Kamal, M. N. A. Khan, K. S. Reddy and K. Rohini, *Bioorg. Med. Chem.*, 2007, **15**, 1004–1013.

11 R. B. Shah, N. N. Valand, P. G. Sutariya and S. K. Menon, *J. Inclusion Phenom. Macrocyclic Chem.*, 2016, **84**, 173–178.

12 M. N. Soares, T. M. Gáscon, F. L. A. Fonseca, K. S. Ferreira and I. A. Bagatin, *Mater. Sci. Eng., C*, 2014, **40**, 260–266.

13 S. Muneer, S. Memon, Q. K. Pahnwar, A. A. Bhatti and T. S. Khokhar, *J. Anal. Sci. Technol.*, 2017, **8**, 3–8.

14 (*a*) L. An, J. Wang, C. Wang, S. S. Zhou, J. Sun and C. G. Yan, *New J. Chem.*, 2018, **10**, 10689–10696; (*b*) Y. Liu, J. Sun and C. G. Yan, *J. Inclusion Phenom. Macrocyclic Chem.*, 2017, **87**, 1–10; (*c*) T. A. Alhujran, L. N. Dawe and P. E. Georghiou, *Org. Lett.*, 2012, **14**, 3530–3533; (*d*) K. Cottet, P. M. Marcos and P. J. Cragg, *Beilstein J. Org. Chem.*, 2012, **8**, 201–226; (*e*) E. A. Shokova and V. V. Kovalev, *Russ. J. Org. Chem.*, 2004, **40**, 607–643; (*f*) B. Masci, *Tetrahedron*, 2001, **57**, 2841–2845; (*g*) G. Brodesser and F. J. Vögtle, *J. Inclusion Phenom. Mol. Recognit. Chem.*, 1994, **19**, 111–135.

15 P. M. Marcos, J. R. Ascenso, M. A. P. Segurado and J. L. C. Pereira, *Tetrahedron*, 2001, **57**, 6977–6984.

16 L. An, H. H. Chen, Z. C. Qin and J. Ding, *Chin. J. Chem. Reagents*, 2009, **20**, 17–19.

17 (*a*) X. Nqoro, N. Tobeka and B. A. Aderibigbe, *Molecules*, 2017, **22**, 2268; (*b*) A. A. Al-Amiery, R. I. Al-Bayati, K. Y. Saour and M. F. Radi, *Res. Chem. Intermed.*, 2012, **38**, 559–569; (*c*) S. Eswaran, A. V. Adhikari, N. K. Pal and I. H. Chowdhury, *Bioorg. Med. Chem. Lett.*, 2010, **20**, 1040–1044; (*d*) S. Kumar, S. Bawa and H. Gupta, *Mini-Rev. Med. Chem.*, 2009, **9**, 1648–1654.

18 K. Abouzid and S. Shouman, *Bioorg. Med. Chem.*, 2008, **16**, 7543–7551.

19 O. Norma, C. John, S. Helen, A. D. K. Hill, M. D. Enda, O. Niall and D. Michael, *Clin. Cancer Res.*, 2003, **9**, 738–742.

20 C. Bavoux, F. Vocanson, M. Perrin and R. Lamartine, *J. Med. Chem.*, 1995, **22**, 119–130.

21 Z. M. Zhao, Y. Wang, J. Han, H. D. Zhu and L. An, *Chem. Pharm. Bull.*, 2015, **63**, 180–186.

22 G. M. Sheldrick, *SHELXL-97, Program for crystal structure refinement*, University of Göttingen, Gottingen, Germany, 1997.